

PAPER • OPEN ACCESS

The impact of film thickness on the properties of ZnO/PVA nanocomposite film

To cite this article: Shaheer Ahmed Khan *et al* 2021 *Mater. Res. Express* **8** 075002

View the [article online](#) for updates and enhancements.



IOP | ebooks™

Bringing together innovative digital publishing with leading authors from the global scientific community.

Start exploring the collection—download the first chapter of every title for free.



PAPER

The impact of film thickness on the properties of ZnO/PVA nanocomposite film

OPEN ACCESS

RECEIVED

31 December 2020

REVISED

9 March 2021

ACCEPTED FOR PUBLICATION

19 March 2021

PUBLISHED

2 July 2021

Original content from this work may be used under the terms of the [Creative Commons Attribution 4.0 licence](#).

Any further distribution of this work must maintain attribution to the author(s) and the title of the work, journal citation and DOI.

Shaheer Ahmed Khan^{1,2,*} , Ataur Rahman² and Fatima Babiker Dafa-Alla Ibrahim³¹ Department of Materials Engineering, NED University of Engineering and Technology (NEDUET), Karachi-75270, Pakistan² Department of Mechanical Engineering, International Islamic University Malaysia (IIUM), Kuala Lumpur-50728, Malaysia³ Department of Biotechnology Engineering, International Islamic University Malaysia (IIUM), Kuala Lumpur-50728, Malaysia

* Author to whom any correspondence should be addressed.

E-mail: shaheer.ahmedkhan@yahoo.com, arat@iium.edu.my and fatimabitumtoog@gmail.com**Keywords:** ZnO/PVA nanocomposite, solution casting, low temperature processing, thickness of ZnO/PVA nanocomposite film**Abstract**

Polymer inorganic nanocomposites are attracting a considerable amount of interest due to their enhanced electrical and optical properties. The inclusion of inorganic nanoparticles into the polymer matrix results in a significant change in the nanocomposite's properties. With this in mind, we have developed a nanocomposite film based on zinc oxide (ZnO) and polyvinyl alcohol (PVA) using a solution casting method with varying concentrations of ZnO nano powder in the PVA matrix. The ZnO / PVA film surface morphology was observed by the scanning electron microscope (SEM). The micrographs indicate that ZnO nanoparticles in the PVA matrix are homogeneously distributed. XRD results indicated that the crystallinity of the film was influenced by the interaction of ZnO nanoparticles and the PVA main chain. Crystallinity is also affected by the doping of ZnO nanoparticles in the PVA matrix and it increases when the concentration of ZnO is low and then decreases when the excess concentration of ZnO is present in the PVA matrix. The FTIR transmission spectra confirmed that significant interaction took place between the ZnO nanoparticles and the PVA main chain over the wave number range of 400–4000 cm⁻¹. The UV–vis spectra reveal that the increase in concentration of ZnO nanoparticles in the polymer matrix results in the movement of the absorption edge in the direction of higher wavelength or lower energy associated with the blue/green portion of the visible spectrum. A decrease in the optical energy bandgap is observed with the increase in nano ZnO concentration in the matrix. Thickness has a significant affect on the properties of the ZnO/PVA nanocomposite and the morphology, particle size, degree of crystallinity and bandgap of the ZnO/PVA nanocomposite samples were influenced by the thickness of the sample. The optimal thickness of 0.03 mm with a weight percentage of 16.6% (ZnO) and 83.3% (PVA matrix) was selected due to its higher bandgap of 4.22 eV, reduced agglomeration/aggregation and smaller ZnO particle size of 14.23 nm in the matrix. The optimal film can be used in photovoltaic research.

1. Introduction

When composites have at least one phase at nanoscale, nanocomposites are made. The power of nanoscale materials maximizes the composite characteristics and can lead to new characteristics. In recent times, great attention has been paid to nanocomposites that contain organic and inorganic phases. The properties of nanoparticles depend not only on the properties of the various components, but also on whether the attractions or compatibility between the two phases are significant and essential [1, 2]. An important application of nanocomposite is in electronics, where thin-film nanocomposites are useful in improving and enhancing the electrical characteristics. Polymer nanocomposites focuses on the final morphology, which depends on interaction between polymer nanoparticles that promote good dispersion and distribution of nanoparticles in the polymer matrix [3, 4].

Zinc oxide is an inorganic compound which has a chemical formula of ZnO. It is an almost insoluble white powder in water. It crystallizes in two primary forms, the hexagonal wurtzite and the cubic zinc mixture [5]. This

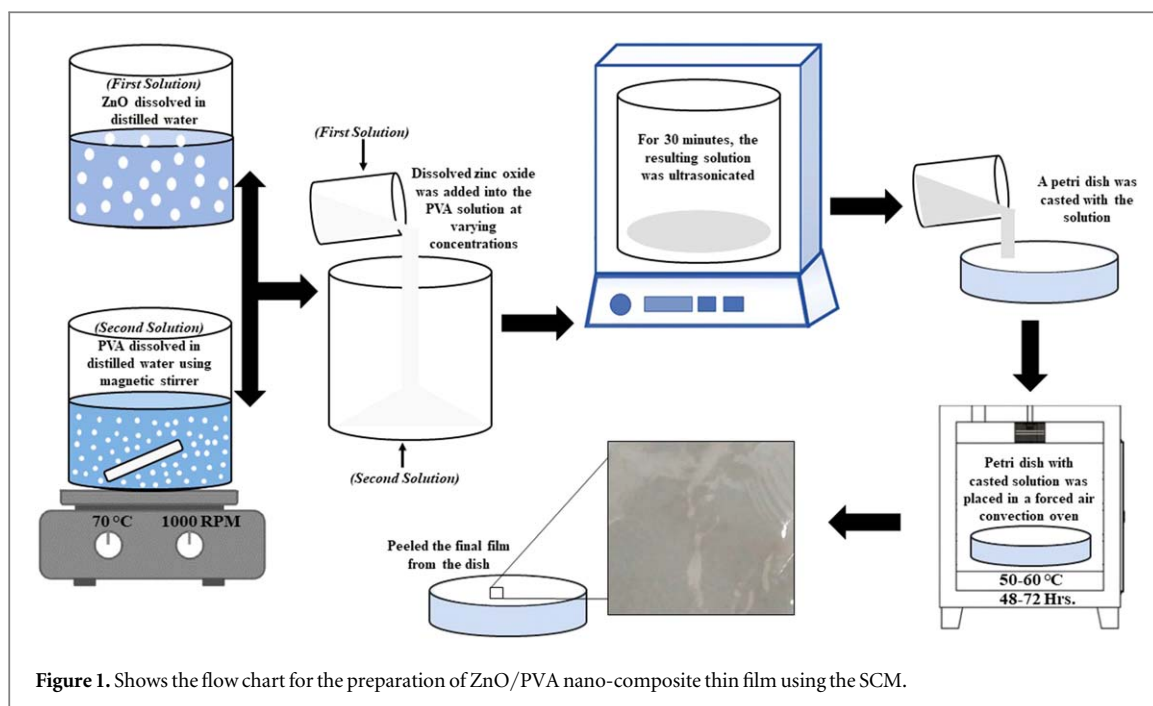


Figure 1. Shows the flow chart for the preparation of ZnO/PVA nano-composite thin film using the SCM.

is a group II—VI semiconductor with approximately 3.33 eV broad band gap. The strong and broad band difference in the near-UV spectral field and the great free exciton binding energy make it a promising functional semiconductor with a wide range of new applications [6]. ZnO has recently been doped with nanoparticles of other materials. By monitoring the dopants and concentrating them, it was determined that the particle's physical properties, such as optical, electrical, and magnetic, could be engineered. That modification and enhancement was obtained because of the electronic structure change and the band gap. Studies are very important in this field for developing applications that can be used in optical devices [7]. ZnO is a technologically important material due to its diverse properties.

PVA is whitish, odorless, non-toxic, biocompatible, thermostable, semi-crystalline or linear synthetic polymer [8, 9]. Poly (vinyl alcohol) (PVA) is also a synthetic water-soluble and biodegradable polymer. Its degradability can be optimized by hydrolysis due to the inclusion of hydroxyl groups. PVA can be dissolved in water for 30 min, with a minimum of ~ 100 °C solvent temperature. The characteristics of polyvinyl acetate depend on the degree or extent of hydrolysis, whether whole or in part. It has a double impact on its classification: partly hydrolyzed and completely hydrolyzed [10]. For completely hydrolyzed and partially hydrolyzed grades, PVA has a melting point of 230 °C and 170 °C–190 °C. It breaks down rapidly above 200 °C because, at high temperatures, it can undergo pyrolysis. It has excellent optical characteristics. Nanofillers with doping can easily change its mechanical, optical, and electrical characteristics. PVA is the perfect matrix for the production of versatile devices in the fields of electronics, optoelectronics, bioengineering, and other areas due to its lack of toxicity, biocompatibility, high hydrophilicity and easy processability. It is therefore very important to adjust the PVA properties for various targeted applications [11].

Various physical and chemical techniques have been used to create, manufacture and obtain the desired ZnO/PVA nanocomposite architecture, such as solvent or solution casting, vapor—liquid—solid growth phase, melt processing, chemical vapor deposition, and *in situ* methods [12]. Different researchers have seen enhanced optical, electrical, thermal, and dielectric properties in ZnO-based PVA nanocomposites prepared by various methods [13–15]. However, any stand-alone paper on the effect of film thickness on the properties of ZnO/ PVA nanocomposite film has not been reported. Therefore, the efforts have been made in this study to find out the optimal thickness of ZnO/PVA nanocomposite film for its possible use in photovoltaic research.

2. Experimental

2.1. Chemicals used

2.1.1. Polymer

Polyvinyl alcohol (PVA) code number 363146 of average mole weight (M_w) 98000 and 99 + % hydrolyzed was used as a polymer and was supplied by Sigma-Aldrich.

Table 1. Composition of total solution of ZnO/PVA mixture.

| Solution (S) | ZnO solution | | PVA stock solution | |
|--------------|------------------------|-------------------------------------|------------------------|-------------------------------------|
| | ZnO _(s) (g) | Deionized water _(l) (ml) | PVA _(s) (g) | Deionized water _(l) (ml) |
| A | 1 | 12 | 2 | 50 |
| B | 4 | 50 | 5 | 100 |
| C | 2.5 | 20 | 4 | 150 |
| D | 3 | 10 | 3 | 75 |

Table 2. Blended mixture of ZnO/PVA with deionized water.

| S. no | Sample from solution ^a | Nanocomposite sample ZnO(ml)PVA(ml) | Sample composition | | Weight percentage | |
|-------|-----------------------------------|-------------------------------------|--------------------|----------|-------------------|---------|
| | | | ZnO (ml) | PVA (ml) | ZnO (%) | PVA (%) |
| 1 | S _A S ₁ | ZnO(1)PVA(5) | 1 | 5 | 16.66 | 83.33 |
| 2 | S _A S ₂ | ZnO(2)PVA(5) | 2 | 5 | 28.57 | 71.42 |
| 3 | S _A S ₃ | ZnO(3)PVA(5) | 3 | 5 | 37.50 | 62.50 |
| 4 | S _B S ₁ | ZnO(5)PVA(5) | 5 | 5 | 50 | 50 |
| 5 | S _A S ₄ | ZnO(1)PVA(6) | 1 | 6 | 14.28 | 85.71 |
| 6 | S _A S ₅ | ZnO(2)PVA(6) | 2 | 6 | 25 | 75 |
| 7 | S _A S ₆ | ZnO(3)PVA(6) | 3 | 6 | 33.33 | 66.66 |
| 8 | S _C S ₁ | ZnO(4)PVA(6) | 4 | 6 | 40 | 60 |
| 9 | S _C S ₂ | ZnO(2)PVA(3) | 2 | 3 | 40 | 60 |
| 10 | S _D S ₁ | ZnO(6)PVA(10) | 6 | 10 | 37.50 | 62.50 |

Notation: ^aS_iS_j; i = A, B, C, D,.....; j = 1,2,3,4,.....

2.1.2. Zinc Oxide (ZnO)

Zinc Oxide (ZnO) was purchased from R&M Chemicals. It was used as a filler in polymer/ZnO nanocomposites. The size of the nanoparticles was < 100 nm (nano-meters and 10×10^{-3} mm) of diameter.

2.1.3. Solvent

Deionized water (H₂O) has no charge (ion free and does not conduct electricity) was used as a solvent for PVA supplied by Sigma-Aldrich. It is a common solvent for this type of polymer. It is a polar protic solvent which structurally has a long hydrocarbon chain.

2.2. Synthesis of ZnO/PVA nanocomposite

The Solution Casting Method (SCM) is an easy and versatile process to develop Nano-composite laboratory scale thin films. In this study, the SCM was used to prepare a laboratory scale thin film of ZnO/PVA Nano-composites. A template (petri dish) has been made with ceramic based on the desired shape (laboratory scale) of the Nano-composite thin film for this study to characterize its composition.

The procedure of preparing the ZnO/PVA nanocomposite is briefly explained in figure 1. The Composition of the total solution of ZnO/PVA mixture and the weight percentages of the blended mixture of ZnO/PVA with deionized water are mentioned in tables 1 and 2, respectively. A total of 10 samples were prepared with different weight percentages of ZnO and PVA.

Different samples of ZnO / PVA Nano-composites with different weight percentages of ZnO and PVA were prepared in order to optimize the sample to obtain a better and more efficient film in terms of thickness, as shown in table 3. The laboratory scale ZnO-PVA Nano-composite thin film has been made based on the size of length \times width (L \times W) of 130 mm \times 60 mm. The thickness of the nanocomposite sample was measured using a digital micrometer. The thickness of different composite films varies from 0.03 mm to 0.10 mm.

2.3. Characterization

A Scanning electron microscope (SEM), Fourier Transform Infrared Spectroscopy (FTIR), X-ray diffraction (XRD), and an UV-visible Spectrophotometer (UV-Vis) were used to characterize the nanocomposite film. The details of the purpose of each test are listed in table 4.

Table 3. Nanocomposite samples.

| Nanocomposite Sample | Thickness (mm) | Sample appearance |
|----------------------|----------------|---|
| ZnO(1)PVA(5) | 0.03 |  |
| ZnO(2)PVA(5) | 0.05 |  |
| ZnO(3)PVA(5) | 0.06 |  |
| ZnO(5)PVA(5) | 0.10 |  |
| ZnO(1)PVA(6) | 0.025 |  |
| ZnO(2)PVA(6) | 0.04 |  |
| ZnO(3)PVA(6) | 0.05 |  |
| ZnO(4)PVA(6) | 0.07 |  |
| ZnO(2)PVA(3) | 0.09 |  |
| ZnO(6)PVA(10) | 0.10 |  |

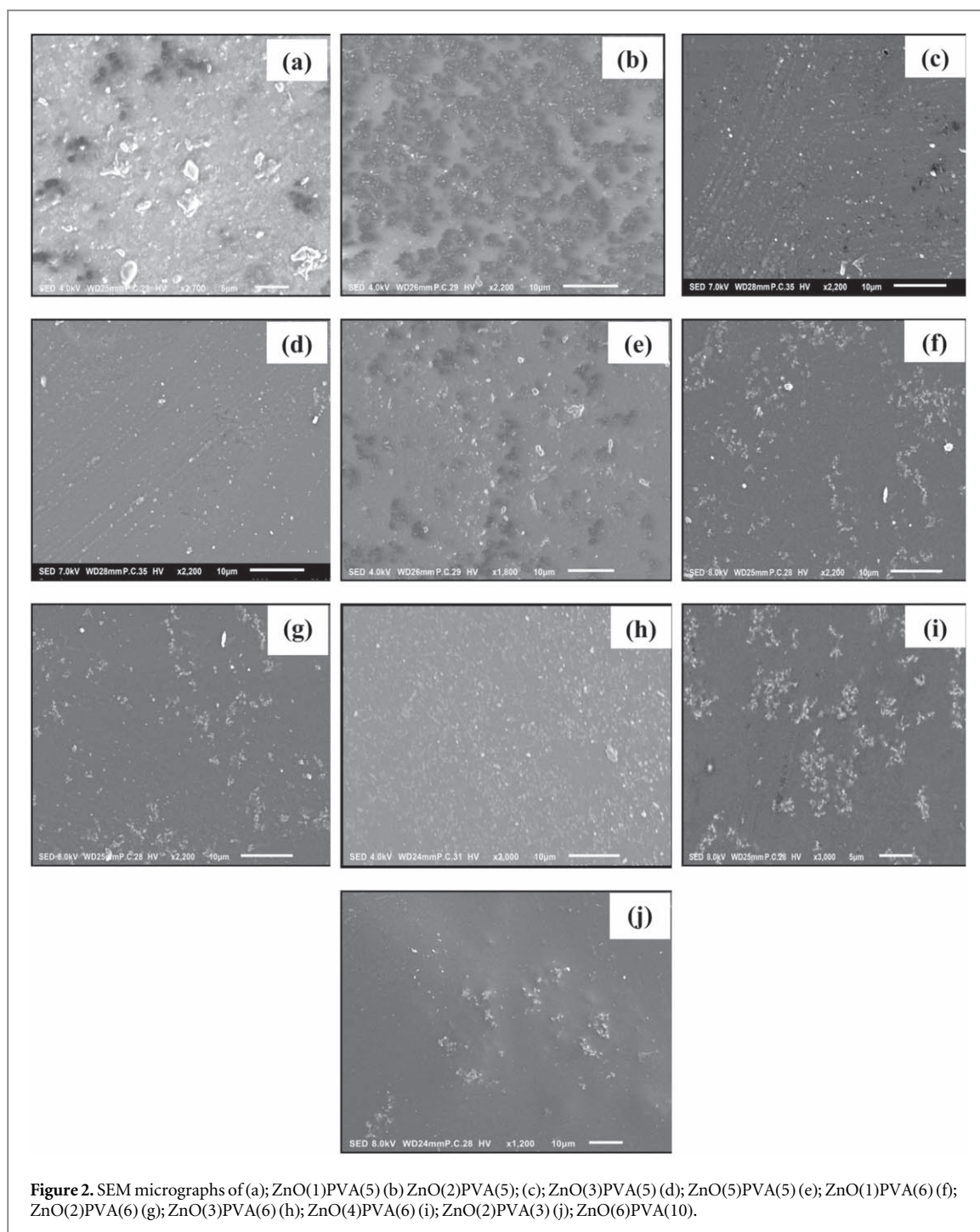


Table 4. Characterization of ZnO/PVA nanocomposite by SEM, FTIR, XRD and UV-vis.

| Machine | Purpose |
|--|---|
| Scanning electron microscope (SEM) | Morphological analysis of the ZnO/PVA Nanocomposite |
| Fourier Transform Infrared Spectroscopy (FTIR) | Observed the presence of functional groups present in ZnO/PVA Nanocomposite |
| X-ray diffraction (XRD) | Examine the diffraction pattern of the ZnO/PVA Nanocomposite |
| UV-visible Spectrophotometer (UV-vis) | Find out the absorption and bandgap of ZnO/PVA Nanocomposite |

3. Results and discussion

A total of 10 samples were selected for characterization. Each sample is characterized using the SEM, FTIR, XRD, and UV-vis Spectrophotometer. The following are the characterization results of each sample.

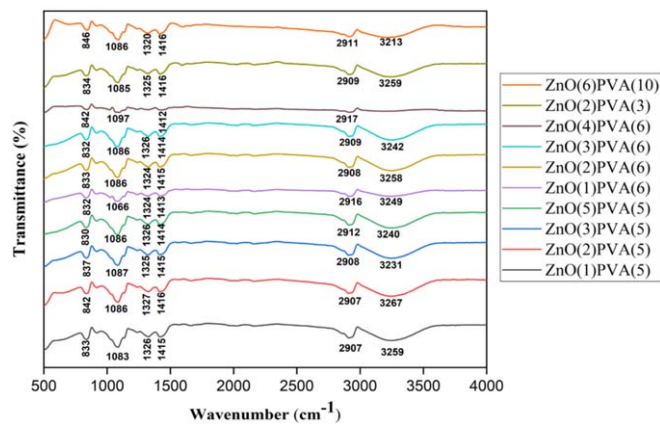


Figure 3. FTIR Transmittance Spectra of nanocomposite samples.

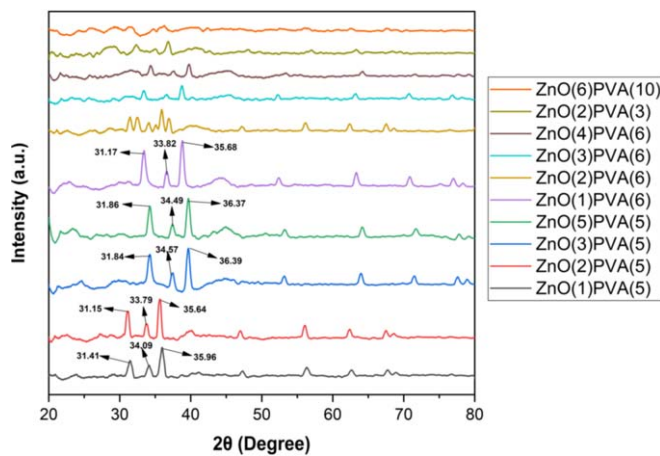


Figure 4. XRD Pattern of nanocomposite samples.

3.1. SEM analysis

The SEM image in figure 2 (a) shows that nano-size crystal aggregates have formed as a result of the high surface energy. However, the micrograph contains several small particles with an average size of 14 nm. The surface morphology study of the ZnO/PVA nano-composite film shows a variety of aggregates or chunks spread randomly on the upper surface of the film. The results indicate that some nano-sized ZnO particles tend to form small aggregates when dispersed in the PVA polymer matrix [16]. The micrograph obtained from prepared film as shown in figure 2(b) examines the homogeneous distribution of nanoparticles in the PVA matrix. The ZnO / PVA nanocomposite showed that crystallites originated and started growing in the immediate surroundings of the surface as the ZnO concentration increased. It also demonstrated homogenous dispersion of ZnO nanoparticles, while there was more compactness and aggregation with increased ZnO concentration [17]. The SEM image of figure 2(c) obtained from prepared films examines the homogeneous distribution of nanoparticles in the PVA matrix. The PVA/ZnO polymer composite film's analysis of surface morphology reveals several aggregates or chunks scattered randomly on the upper surface of the film. It is important to note that irregular ZnO nanoparticles have been formed in the range of 15 nm to 18 nm. The micrograph of figure 2(d) shows a uniformly processed smooth PVA matrix with chunks of flaked shaped ZnO particles distributed over the surface. It is important to note that irregular ZnO nanoparticles have been formed in the range of 16 nm to 19 nm. Figure 2 (e) shows an SEM image of a uniformly processed smooth PVA matrix with an irregular shape and large ZnO particles. Compactness is observed in the image due to the increase in the concentration of ZnO particles in the polymer matrix. Figure 2(f) shows the ZnO particles consist of agglomerating several primary crystallites with an irregular size and shape. Compactness occurs at different points as the ZnO concentration increases, suggesting the sample's more crystalline nature. Figure 2(g) depicts a pure PVA film with non-uniform solution dispersion due to improper drying or more porosity in the final mixture. Compactness occurs at different points as the ZnO concentration increases, suggesting the sample's more crystalline nature. The ZnO/PVA composite micrograph as shown in figure 2(h) confirms improvements

in PVA morphology with ZnO dispersion into the polymer matrix. It displays evenly distributed nano ZnO where there is more compactness as the dopant concentration increases. The micrograph in figure 2(i) shows the ZnO/PVA film with more concentration of PVA in the matrix, resulting in the improper mixing of the ZnO. The micrograph in figure 2(j) shows the highly irregular ZnO/PVA film with large area affected by the high temperature or longer drying time of the oven.

3.2. FTIR analysis

Figure 3 shows the FTIR spectra of ten samples ranging from ZnO (1) PVA (5) to ZnO (6) PVA (10) with a wide absorption peak at 3259, 3267, 3231, 3240, 3249, 3258, 3242, 3207, 3259, and 3213 cm^{-1} , respectively. The band allocated to 2907, 2907, 2908, 2912, 2916, 2908, 2909, 2917, 2909, and 2911 cm^{-1} , respectively, displays C-H asymmetric stretching vibrations. Absorbance at (1415, 1326 cm^{-1}), (1416, 1327 cm^{-1}), (1415, 1325 cm^{-1}), (1414, 1326 cm^{-1}), (1413, 1324 cm^{-1}), (1415, 1324 cm^{-1}), (1414, 1326 cm^{-1}), (1412 cm^{-1}), (1416, 1325 cm^{-1}), (1416, 1320 cm^{-1}), associated with CH_2 vibrations. The strong band at 1083, 1086, 1087, 1086, 1066, 1086, 1086, 1097, 1085, 1086 cm^{-1} , respectively, correlates to the C–O stretching of the PVA matrix acetyl group [18]. The shift in the spectra could be the result of the creation of intermolecular hydrogen bonding between the OH group of PVA with the ZnO surface. The change in the associated doping bands indicates interaction between PVA and ZnO. Higher ZnO concentrations in the PVA matrix exhibit a different behaviour than lower ZnO concentrations in the PVA matrix because increasing ZnO concentrations cause agglomeration of ZnO nanoparticles, reducing the amount of surface atoms and involvement in both the ZnO nanoparticles and polymer matrix.

3.3. XRD analysis

Figure 4 depicts the XRD patterns of 9 samples of ZnO / PVA Nanocomposite from ZnO(1)PVA(5) to ZnO(2) PVA(3), displays a relatively high peak of $2\theta = 35.96, 35.64, 36.39, 36.37, 35.68, 35.91, 35.66, 36.47, 36.78$. The related diffraction peaks corresponded to the PVA diffraction peak and the regular ZnO wurtzite hexagonal crystal structure PDF database (JCPDS 36–1451) [19]. The formation of the ZnO/PVA nanocomposite has been confirmed by these diffraction peaks. By employing the Debye–Scherrer formula, the crystallite size of 9 samples of PVA / ZnO nanocomposite film was measured as shown in table 5. Doping of ZnO nanoparticles results in an increase in crystallinity, but excessive doping of ZnO nanoparticles results in a decrease in crystallinity due to variability in crystalline size and aggregate formation. Contractions in peak width and the sharpness of peaks show the growth in grain size. There has been a rise in strain in the nanocomposite films due to PVA's matrix effect on the ZnO nanocrystals.

The XRD pattern of ZnO(6)PVA(10) sample peaks did not match with the PVA diffraction peak and the regular ZnO wurtzite hexagonal crystal structure PDF database (JCPDS 36-1451). There is no sharp peak observed in the pattern due to which crystallite size of ZnO/PVA nanocomposite films cannot be calculated using Debye–Scherrer formula.

3.4. UV–vis Spectrophotometer

Figure 5 shows the absorption spectra of 10 samples of ZnO / PVA Nanocomposite from ZnO(1)PVA(5) to ZnO (6)PVA(10) display two bands at (235, 356 nm), (225, 340 nm), (234, 335 nm), (239, 339 nm), (235, 366 nm), (258, 340 nm), (250, 341 nm), (262, 367 nm), (238, 356 nm), (227, 330 nm), respectively with a lower intensity corresponding to the existence of ZnO in the film [20]. These bands are attributed to PVA absorption and ZnO nanoparticle excitons. The energy bandgap is found by converting the spectrum into Tauc's plot as shown in figure 6. The increase in concentration of ZnO nanoparticles in the polymer matrix results in the movement of the absorption edge in the direction of higher wavelength or lower energy associated with the blue/green portion of the visible spectrum. Decrease in optical energy bandgap is observed with the increase of nano ZnO concentration into the matrix. The observed shift in energy could be due to the Burstein–Moss phenomenon and the formation of microstrain in the ZnO/PVA nanocomposite. Strain also causes variation in the energy band structure of the ZnO dopant, as shown by a change in the absorption edge. Additionally, the ZnO causes formation of more defects in band gap could be another reason for the shift.

The selected 10 samples were prepared based on different stock solutions, the details of which are mentioned in table 2. These samples were characterized by using SEM, FTIR, XRD and UV–vis. The results obtained are briefly listed in table 6. It can be seen from SEM results, the agglomeration/aggregation in ZnO/PVA nanocomposite increased by the addition of ZnO nanoparticles in PVA matrix from ZnO(1)PVA(5) to ZnO(5) PVA(5); ZnO(1)PVA(6) to ZnO(2)PVA(3). This is due to the creation of clusters on different points of the surface due to high surface energy. When the concentration of ZnO is up to 37.5 wt.%, the degree of crystallinity increases from ZnO(1)PVA(5) to ZnO(3)PVA(5); ZnO(1)PVA(6) to ZnO(2)PVA(3) and then it decreases until 50 wt.%. UV–vis results illustrate the energy bandgap decreases with the increase of ZnO concentration in

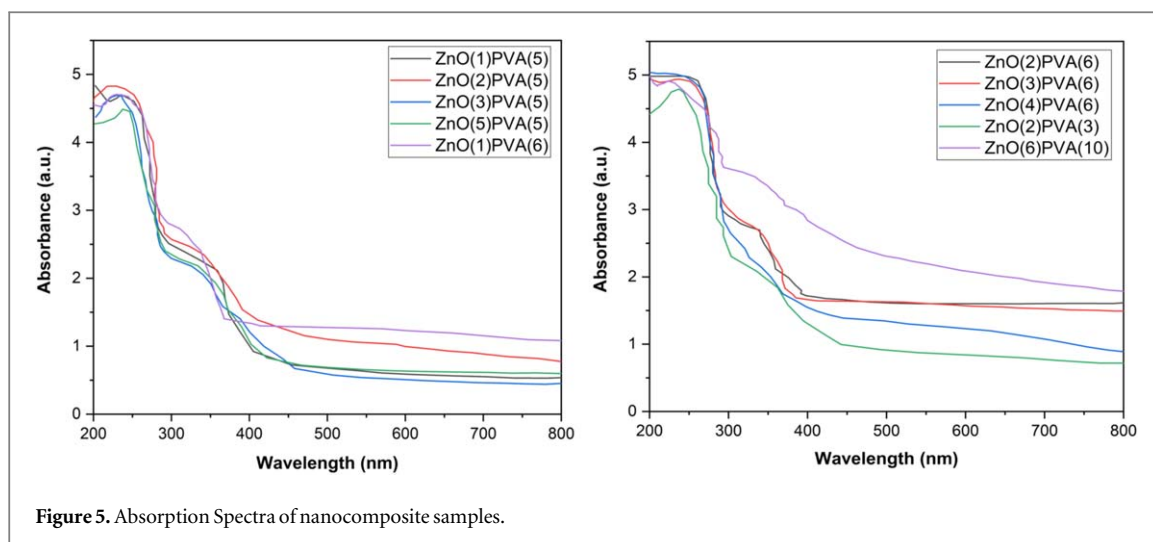


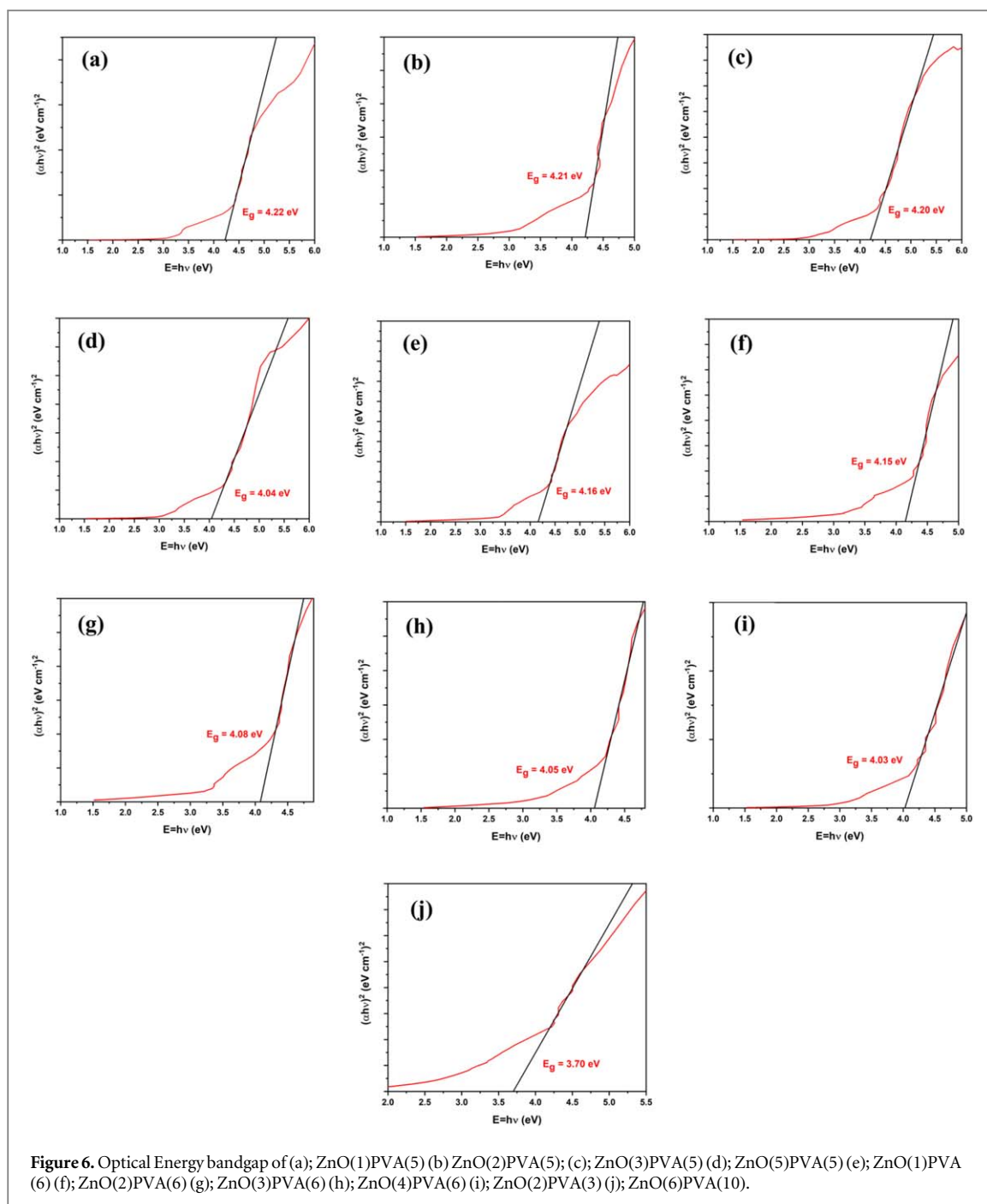
Figure 5. Absorption Spectra of nanocomposite samples.

Table 5. Lattice parameters from XRD pattern.

| Nanocomposite sample | Miller indices (hkl) | Peak position 2θ | FWHM β | D = $K\lambda/\beta\cos\theta$ (nm) | Interplanar spacing d (Å) | Lattice parameter a | Lattice parameter c | Avg. particle Size |
|----------------------|----------------------|-------------------------|--------------|-------------------------------------|---------------------------|---------------------|---------------------|-------------------------------------|
| | | | | | | | | D = $K\lambda/\beta\cos\theta$ (nm) |
| ZnO(1)PVA(5) | (100) | 31.41 | 0.57 | 14.28 | 2.8457 | 3.2859 | 5.2558 | 14.23 |
| | (002) | 34.09 | 0.58 | 14.22 | 2.6279 | | | |
| | (101) | 35.96 | 0.58 | 14.19 | 2.4954 | | | |
| ZnO(2)PVA(5) | (100) | 31.15 | 0.50 | 16.37 | 2.8689 | 3.3127 | 5.3011 | 17 |
| | (002) | 33.79 | 0.49 | 16.79 | 2.6505 | | | |
| | (101) | 35.64 | 0.46 | 17.84 | 2.5170 | | | |
| ZnO(3)PVA(5) | (100) | 31.84 | 0.53 | 15.45 | 2.8082 | 3.2427 | 5.1850 | 17 |
| | (002) | 34.57 | 0.44 | 18.79 | 2.5925 | | | |
| | (101) | 36.39 | 0.48 | 17.37 | 2.4669 | | | |
| ZnO(5)PVA(5) | (100) | 31.86 | 0.48 | 16.86 | 2.8065 | 3.2407 | 5.1966 | 18.31 |
| | (002) | 34.49 | 0.42 | 19.55 | 2.5983 | | | |
| | (101) | 36.37 | 0.45 | 18.54 | 2.4682 | | | |
| ZnO(1)PVA(6) | (100) | 31.17 | 0.52 | 15.81 | 2.8671 | 3.3106 | 5.2965 | 18.93 |
| | (002) | 33.82 | 0.37 | 22.13 | 2.6482 | | | |
| | (101) | 35.68 | 0.44 | 18.85 | 2.5143 | | | |
| ZnO(2)PVA(6) | (100) | 31.46 | 0.47 | 17.39 | 2.8413 | 3.2808 | 5.5088 | 16.94 |
| | (002) | 32.48 | 0.52 | 15.89 | 2.7544 | | | |
| | (101) | 35.91 | 0.47 | 17.56 | 2.4987 | | | |
| ZnO(3)PVA(6) | (100) | 31.13 | 0.39 | 20.78 | 2.8707 | 3.3148 | 5.2874 | 18.02 |
| | (002) | 33.88 | 0.51 | 16.11 | 2.6437 | | | |
| | (101) | 35.66 | 0.39 | 21.14 | 2.5157 | | | |
| ZnO(4)PVA(6) | (100) | 31.96 | 0.46 | 17.71 | 2.7980 | 3.2308 | 4.9233 | 19.34 |
| | (002) | 36.47 | 0.41 | 20.15 | 2.4616 | | | |
| | (101) | 56.86 | 0.55 | 16.21 | 2.2062 | | | |
| ZnO(2)PVA(3) | (100) | 36.78 | 0.57 | 14.58 | 2.4416 | 2.8193 | — | 14.58 |
| | (002) | — | — | — | — | | | |
| | (101) | — | — | — | — | | | |
| ZnO(6)PVA(10) | (100) | — | — | — | — | — | — | — |
| | (002) | — | — | — | — | | | |
| | (101) | — | — | — | — | | | |

matrix from ZnO(1)PVA(5) to ZnO(6)PVA(10). The thickness of the ZnO/PVA nanocomposite film increases with the decrease in the optical bandgap of the ZnO/PVA nanocomposite film.

The performance of sample ZnO(1)PVA(5) comparable to other samples shows less agglomeration/aggregation and smaller ZnO particle size of 14.23 nm. It also shows a high energy bandgap of 4.22 eV by converting the spectra into Tauc's Plot, which is higher than the other samples made in this study using the



nano-powder of ZnO and PVA. The sample ZnO(1)PVA(5) with a weight percentage (16.66 wt.%) of ZnO and (83.33 wt.%) of PVA and a thickness of 0.03 mm is found to be optimal and is suggested for the further possible application in photovoltaic research.

4. Conclusion

In summary, different samples of ZnO/PVA nanocomposite were successfully prepared by the solution casting method. Each sample was characterized by SEM, XRD, FTIR and UV-vis and the results of each sample were briefly discussed. The findings revealed that the morphology, particle size, degree of crystallinity and bandgap of the ZnO/PVA nanocomposite film samples were affected by the thickness of the sample. The sample ZnO(1)PVA(5) has an optimal thickness of 0.03 mm because of its optimum value of 4.22 eV bandgap and less agglomeration/aggregation of 14.23 nm particles. A thin film of ZnO/PVA nanocomposite with optimal thickness can be applied in photovoltaic research due to its fascinating properties. However, future study on

Table 6. Summarized characteristics result.

| No. | Sample Description (Listed according to increasing ZnO wt.%) | Characteristics result | | | | Energy band gap (E_g), eV |
|-----|--|------------------------|--|------------------|---------------------|-------------------------------|
| | | SEM ^a | FTIR ^b | XRD ^c | UV-vis ^d | |
| 1 | ZnO(1)PVA(5) | ↑ | (C-H: 2907); (CH ₂ : 1415, 1326); (C-O: 1083) | 14.23 nm (↑) | 235 nm, 356 nm | 4.22 |
| 2 | ZnO(2)PVA(5) | ↑↑ | (C-H: 2907); (CH ₂ : 1416, 1327); (C-O: 1086) | 17 nm (↑↑) | 225 nm, 340 nm | 4.21 |
| 3 | ZnO(3)PVA(5) | ↑↑↑ | (C-H: 2908); (CH ₂ : 1415, 1325); (C-O: 1087) | 17 nm (↑↑↑) | 234 nm, 335 nm | 4.20 |
| 4 | ZnO(5)PVA(5) | ↑↑↑↑ | (C-H: 2912); (CH ₂ : 1414, 1326); (C-O: 1086) | 18.31 nm (↑↑) | 239 nm, 339 nm | 4.04 |
| 5 | ZnO(1)PVA(6) | ↑↑ | (C-H: 2916); (CH ₂ : 1413, 1324); (C-O: 1066) | 18.93 nm (↑) | 235 nm, 366 nm | 4.16 |
| 6 | ZnO(2)PVA(6) | ↑↑↑ | (C-H: 2908); (CH ₂ : 1415, 1324); (C-O: 1086) | 16.94 nm (↑↑) | 258 nm, 340 nm | 4.15 |
| 7 | ZnO(3)PVA(6) | ↑↑↑↑ | (C-H: 2909); (CH ₂ : 1414, 1326); (C-O: 1086) | 18.02 nm (↑↑↑) | 250 nm, 341 nm | 4.08 |
| 8 | ZnO(4)PVA(6) | ↑↑↑↑↑ | (C-H: 2917); (CH ₂ : 1412); (C-O: 1097) | 19.34 nm (↑↑) | 262 nm, 367 nm | 4.05 |
| 9 | ZnO(2)PVA(3) | ↑↑↑↑↑↑↑ | (C-H: 2909); (CH ₂ : 1416, 1325); (C-O: 1085) | 14.58 nm (—) | 238 nm, 356 nm | 4.03 |
| 10 | ZnO(6)PVA(10) | — | (C-H: 2911); (CH ₂ : 1416, 1320); (C-O: 1086) | (—) | 227 nm, 330 nm | 3.70 |

^a SEM: Agglomeration/Aggregation of particles (↑)

^b FTIR: C-H, CH₂, C-O (cm⁻¹)

^c XRD: average particle size (nm), degree of crystallinity (↑)

^d UV-vis: Absorption (nm).

fabrication aspects of ZnO/PVA nanocomposites could be carried out for further improvement and investigation into their long-lasting use in photovoltaic research.

Data availability statement

All data that support the findings of this study are included within the article (and any supplementary files).

ORCID iDs

Shaheer Ahmed Khan  <https://orcid.org/0000-0002-7302-0884>

References

- [1] Shah Mutabar, Khan Noman, Imran Zahid, Khan Masood, Khattak Abraiz, Khan Adam and Ullah Naimat 2019 Structural, optical and impedance spectroscopy study of thin film of polyaniline (PANI/ZnO) nanocomposite *Materials Research Express* **7** 01534
- [2] Khan Shaheer A. and Rahman Aatur 2019 Efficiency of thin film photovoltaic paint: A brief review *International Journal of Recent Engineering and Technology* **7** 163–9 Available at: <https://www.ijrte.org/wp-content/uploads/papers/v7i6s/F02330376S19.pdf>
- [3] Soares I L, Chimanowsky J P, Luetkmeyer L, Silva E O D, Souza D D H S and Tavares M I B 2015 Evaluation of the influence of modified TiO₂ particles on polypropylene composites *J. Nanosci. Nanotechnol.* **15** 5723–32
- [4] Rahman Aatur, Aung Kaw Myo and Khan Shaheer Ahmed 2020 Organic Photoelectric-Supercapacitor Power Source of Electric Vehicle *TEST Engineering and Management* **82** 15175–82 Available at: <http://testmagazine.biz/index.php/testmagazine/article/view/3231/2854>
- [5] Rahman Aatur, Aung Kaw Myo, Saifullah Khalid and Rahman Mizanur 2017 Physics of ZnO/SiO₂ electrolyte semi-conductive thermal electric generator *International Journal of Advanced and Applied Sciences* **4** 35–40
- [6] Liu R 2014 Hybrid organic/inorganic nanocomposites for photovoltaic cells *Materials* **7** 2747–71
- [7] Shanshool H M, Yahaya M, Yunus W M M and Abdullah I Y 2016 Investigation of energy band gap in polymer/ZnO nanocomposites *J. Mater. Sci., Mater. Electron.* **27** 9804–11
- [8] Abdullah Z W, Dong Y, Davies I J and Barbhuiya S 2017 PVA, PVA blends, and their nanocomposites for biodegradable packaging application *Polym.-Plast. Technol. Eng.* **56** 1307–44
- [9] Saini I, Sharma A, Dhiman R, Aggarwal S, Ram S and Sharma P K 2017 Grafted SiC nanocrystals: For enhanced optical, electrical and mechanical properties of polyvinyl alcohol *J. Alloys Compd.* **714** 172–80
- [10] Verma R 2018 *Design, fabrication and characterization of PVA/Nanocarbon composite fibers* Arizona State University (Order No. 10981635). Available from ProQuest Dissertations & Theses Global. (2154886070). Retrieved from (<http://210.48.222.80/proxy.pac/docview/2154886070?accountid=44024>)
- [11] Awada H and Daneault C 2015 Chemical modification of poly (vinyl alcohol) in water *Applied Sciences* **5** 840–50
- [12] Koo J H 2016 Mechanical properties of polymer nanocomposites *Fundamentals, Properties, and Applications of Polymer Nanocomposites* (Cambridge, UK: Cambridge University Press) 273–331
- [13] Hemalatha K S, Rukmani K, Suriyamurthy N and Nagabhushana B M 2014 Synthesis, characterization and optical properties of hybrid PVA–ZnO nanocomposite: a composition dependent study *Mater. Res. Bull.* **51** 438–46
- [14] Mohammed N, Rasheed Z and Hassan A 2019 Improvement Optical Properties of PVA/ TiO₂ and PVA/ ZnO Nanocomposites *Al-Mustansiriyah Journal of Science* **29** 118
- [15] Rahman Aatur and Kibria Golam 2021 Energy storage Al-ZnO/CuO_CFRP organic structural auxiliary energy storage system for electric vehicle *Solid State Science and Technology* **28** 103–16 Available at: <http://myjms.mohe.gov.my/index.php/masshp/article/view/10739>
- [16] Kumar N. B. Rithin, Crasta Vincent and Praveen B. M. 2014 Advancement in Microstructural, Optical, and Mechanical Properties of PVA (Mowiol 10-98) Doped by ZnO Nanoparticles *Physics Research International* **1** 1–9
- [17] Kandulna R and Choudhary R B 2018 Concentration-dependent behaviors of ZnO-reinforced PVA–ZnO nanocomposites as electron transport materials for OLED application *Polym. Bull.* **75** 3089–107
- [18] Ambrosio Roberto, Carrillo Amanda, Mota Maria L, de la Torre Karla, Torrealba Richard, Moreno Mario, Vazquez Hector, Flores Javier and Vivaldo Israel 2018 Polymeric Nanocomposites Membranes with High Permittivity Based on PVA-ZnO Nanoparticles for Potential Applications in Flexible Electronics *Polymers* **10** 1370
- [19] Viswanath V, Nair S S, G. S and Muneera C.I. 2019 Zinc oxide encapsulated poly (vinyl alcohol) nanocomposite films as an efficient third-order nonlinear optical material: Structure, microstructure, emission and intense low threshold optical limiting properties *Materials Research Bulletin* **112** 281–91
- [20] Fernandes D.M., Silva R., Hechenleitner A.A.W, Radovanovic E., Melo M.A.C and Pineda E A G 2009 Synthesis and characterization of ZnO, CuO and a mixed Zn and Cu oxide *Materials Chemistry and Physics* **115** 110–15